JOURNAL OF AIRCRAFT
Vol. 47, No. 5, September–October 2010

Evaluation of the Thrust Recovery of an Aircraft Flapped Outflow Valve

Xavier Carbonneau,* Nicolas Binder,* and Stéphane Jamme*
Université de Toulouse, F-31055 Toulouse Cedex 4, France

DOI: 10.2514/1.47419

This paper presents a detailed study of a flapped outflow valve. Well-known as part of the pressurization system of aircraft, this type of valve is also designed for thrust recovery even if the efficiency of the system has never been demonstrated. A ground experimental test rig is first designed to provide global and local measurements to be used as validation data for numerical simulations. Once the validation of the numerical approach is achieved on a ground configuration, additional three-dimensional computations are then conducted for cruise conditions. They lead to a reliable estimation of thrust recovery as well as interesting insight in the aerodynamic behavior of the flow across the valve and its associated three-dimensional effects.

Nomenclature

F	=	thrust
P	=	pressure
P_{Rc}	=	cabin pressure ratio
Q	=	mass flow
Q_r	=	reduced mass flow
R	=	perfect gas constant
S	=	geometric section area
T	=	temperature
V	=	velocity
γ	=	specific heat ratio
ξ	=	nozzle mean line angle from horizontal direction
ρ	=	density

Subscripts

c	=	cabin location
e	=	external location
ref	=	reference conditions
s	=	static conditions
t	=	total conditions or throat

I. Introduction

THE outflow valve is an aircraft equipment devoted to the pressurization system. It insures the pressure regulation of the cabin to a value equivalent to 8000–10,000 ft of altitude, when the actual cruise altitude is about 25,000–30,000 ft.

Two families of outflow valves can be distinguished. The first one is the butterfly-outflow valve [1] and has been widely studied (see, e.g., Fejtek et al. [2]). Its main drawback has been highlighted: a fully 3-D turbulent flow is generated through its circular shape. A large amount of inlet energy is thus lost and because of the complex flowfield generated, it cannot be pitched on the skin of the aircraft. The second one is the flapped outflow valve [3,4]. The control of pressurization is done by the rotation of two flaps, to adapt a nozzle geometry to the pressure ratio specified during the whole flight. The flapped outflow valve generates a rectangular jet where velocities can reach low supersonic levels (Mach number 1.5) at nominal operating conditions. Provided that this jet is properly located and oriented on the skin of the aircraft, it is likely to generate a thrust. The most recent studies have concentrated on acoustic studies [5] because much noise is associated to the transonic jet produced. But even if the pressurization function is fully satisfied, the real thrust recovery potential of the system has never been demonstrated. To quantify the order of magnitude of the thrust recovered some flight tests were conducted by aircraft manufacturers. The thrust component generated by the flapped-valve was estimated from the fuel consumption measurements without a real accuracy.

As presented in Figs. 1 and 2, the aircraft outflow valve is the interface between two domains. The airflow in the domain (1), called *cabin*, is driven through the valve to external freestream of different temperature and pressure domain (2). In Fig. 1, the valve is located at the beginning of the upsweep. It is generally the case, but this equipment can also be found either on the rear side of the aircraft or near the landing gear. The pressure regulation inside the cabin depends not only on the altitude but also on the amount of air ejected (i.e., the exhaust mass flow). The flaps of the valve are controlled by an actuator, which corrects the external pressure variations or mass flow fluctuations (the air cabin is supplied by the engines), to maintain a specified pressure level. The configuration of the valve moves from fully opened, before takeoff, to nominal opening in cruise flight conditions. At cruise conditions the flaps position is optimum in terms of shape continuity with the skin of the aircraft. The cruise configuration is set to induce sonic conditions at the throat section of the nozzle, leading to a possible supersonic jet expansion downstream (depending on the external pressure level). The force generated by the jet is called the recovered thrust. A theoretical nozzle calculation can give an estimation of this recovered thrust: based on the valve dedicated to a 100-seat airplane class, for nominal operating conditions, the thrust induced should be 155 N (using a 1-D approximation and considering a basic specific fuel consumption of 0.7 (kg/daN/hr), for a 10 h flight, the equivalent of fuel mass is 108 kg). But this rough estimation is very difficult to verify at operating conditions, and the real effect of this equipment in terms of thrust recovery is still not fully identified.

The airflow of the present exhaust valve and its complex mixing with the external freestream is poorly described in the literature, even if the phenomena linked to supersonic jet mixing have been widely studied. Dash and Wolf [6,7] give a complete picture of this phenomenology. Others studies describe the 3-D problem of interaction of supersonic jet in subsonic compressible crossflow [8–10]. In this configuration, the specificity of rectangular jets developments are discussed in Plesniak and Cusano [11] or Weston and Thames [12] for instance. They point out a dependency of the phenomenologies to the external flow Mach number, associated with large transverse 3-D structures. At different degrees, most of the configurations studied induce the development of strong tridimensional vortex at the exit of the cross jet. Even if the flow configuration presented herein is quite different because of a small deviation

Received 19 October 2009; revision received 13 March 2010; accepted for publication 27 April 2010.

*Associate-Professor, ISAE, 10 Avenue Edouard Belin, BP 54032.

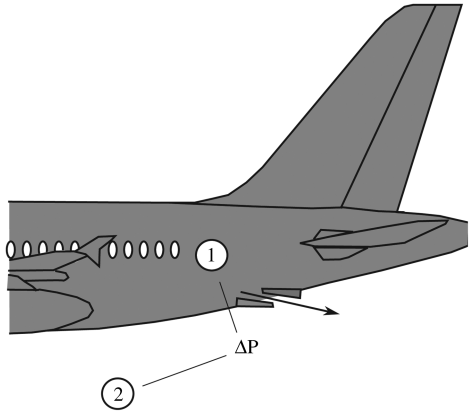

Fig. 1 Airflow domains presentation.

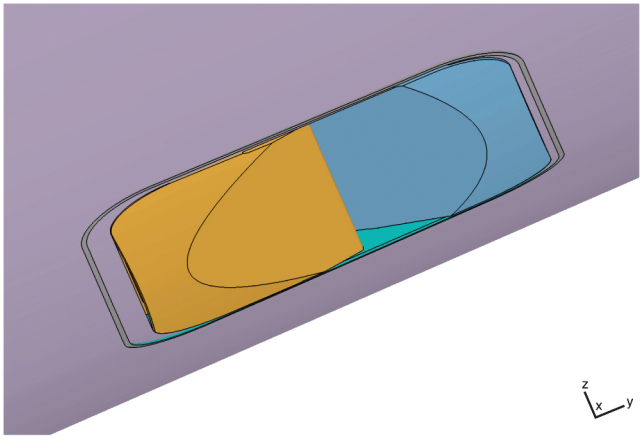

Fig. 2 Outflow valve flaps.

imposed between the jet and the external flow, side effects are expected due to the thick flaps edges (Fig. 3).

The purpose of the present study is to determine the actual thrust recovery potential of a flapped outflow valve at cruise conditions. The choice has been made to proceed with 2-D and 3-D computational fluid dynamics (CFD) analysis to compute the thrust recovery because it is delicate to build a relevant test device in real operating conditions (especially the external flow Mach number). However, the thrust estimation on some unusual flow configurations such as the one expected (large aspect ratio supersonic jet in a high subsonic external flow near an aircraft cabin wall) is not an easy CFD process an needs validation. A specific ground test device has thus been designed to provide the experimental information allowing a reliable computation of the thrust. This experiment is in no way representative of real flight conditions, but will attest the ability of CFD to predict a good thrust value in highly tridimensional transonic flows. The paper is organized following the steps of the approach: we first describe the experimental device and the results obtained. CFD calculation are then presented and the fastidious process of the validation of the thrust estimation is also detailed. In the last section of the paper, the determination of the thrust recovery is presented and discussed, together with some description of the flow pattern with an emphasis on the observed tip effects.

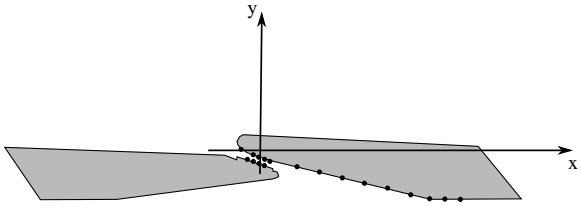

Fig. 3 Position of the local pressure measurements on the valve.

II. Experimental Approach

A. Experimental Facility and Instrumentation

A specific test rig has been designed for validation of the numerical computation of the effective thrust generated. Its requirements are the production of a transonic jet in a low-velocity field, with pressure levels as small as possible, for safety reasons. Even if the purpose of the bench is not the simulation of the actual inflight conditions, a real outflow valve has been used to produce the supersonic jet. Its electric actuator allows setting the opening configuration. Figure 4 shows the details of the global instrumentation. The pressurized air is driven to a cubic box (hereafter called *cabin*) through a flexible pipe in vertical position (not to affect the thrust measurement). The mean inlet cabin pressure and temperature are measured at the pipe outlet. External pressure and temperature are acquired simultaneously. The cabin can move along the axial (or thrust) direction x because it is suspended with four thin steel hangers. A compression load cell with a rated capacity of 500 N gives the thrust value. The geometry of the external face of the box representing the skin of the aircraft has been adapted to match exactly the curved shape of the valve frame.

The flow operating conditions have been defined to reach sonic velocity at the throat section of the channel between the flaps. The exhaust conditions are ambient pressure and temperature without external velocity. The supposed optimal opening position of the valve has been chosen and a pressure ratio across the outflow valve of $P_{tc}/P_e = 1.5$ has been imposed. This value is smaller by half compared with the real flight conditions, but produces the desired supersonic jet with a reasonable pressure level in the box simulating the cabin.

The outflow valve tested is a real equipment devoted to pressurization. The pressure regulation does not involve the throat section area as an active parameter of the valve operating control. Thus, the knowledge of this section is not perfect. An estimated value is available by calibration, which can be verified before and after tests, but not during the experimentations. An indirect measurement can, however, be made by using the mass flow rate value across the valve. Because the throat section of the valve is effectively choked, the mass flow rate at a sonic section can be written as:

$$Q = S_t \sqrt{\frac{\gamma}{R}} \frac{P_t}{\sqrt{T_t}} \left(\frac{\gamma + 1}{2} \right)^{\frac{-(\gamma+1)}{2(\gamma-1)}} \tag{1}$$

The Eq. (1) shows that the mass flow rate is a linear function of the section area. A differential pressure flowmeter has thus been installed upstream of the cabin and allows deducing the throat effective section area.

In addition to the global measurements previously described, the local static pressure distribution on the flaps of the valve is measured by 18 pressure transducers connected on 18 holes (diameter of 0.5 mm: 4 and 14 on the upstream and the downstream flaps, respectively). All transducers measurements are relative to atmospheric pressure. The specifications are detailed in Table 1.

B. Data Obtained

This section focuses on the main experimental results gathered during this work, and the verification of the bench ability to produce a

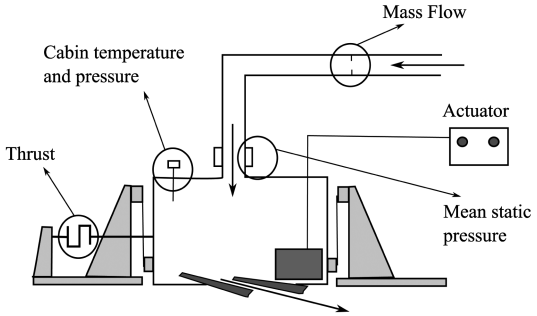

Fig. 4 Details of the global instrumentation.

Table 1 Pressure transducers specifications

Characteristics	Cabin pressure	Flaps pressure	Thrust	Mass flow
Range	0/1 bar	−0.4/0.6 bar	0/500 N	0/500 g/s
Error	±1 mbar	±0.1 mbar	±2.5 N	±10 g/s

transonic jet. We first analyze the global parameters, and then the local pressure measurements will be presented. The opening configuration is denominated according to the height measured at the throat section of the channel between the flaps. As stated before, the design cruise opening is 100%. Four additional opening values have also been tested, namely 50, 75, 125, and 150%.

Figure 5 presents the evolution of the reduced mass flow rate Q_r as a function of the cabin pressure ratio P_{Rc}. These two parameters are defined as follows:

$$Q_r = Q\sqrt{\frac{T_{tc}}{T_{\text{ref}}}}\frac{P_{\text{ref}}}{P_{tc}} \quad \text{and} \quad P_{Rc} = \frac{P_{tc}}{P_e} \quad \text{with} \quad P_{\text{ref}} = 101325 \text{ Pa}$$

$$\text{and} \quad T_{\text{ref}} = 288 \text{ K} \tag{2}$$

As expected, Q_r increases with P_{Rc} up to choked conditions at throat. The plateau observed on the curves associated to the three low opening configurations of the valve (50, 75, and 100%) shows the blockage of the channel, and confirms the transonic nature of the jet. It can be verified that the operating point defined as the reference for the nominal opening ($P_{Rc} = 1.5$) is situated on the plateau. Sonic conditions are thus guaranteed at this specific point which will also be the reference for validation.

Figure 6 shows that the thrust F increases almost linearly with the pressure ratio. For the reference operating conditions (opening 100% and $P_{Rc} = 1.5$), the thrust reaches a value of 9 daN. Figure 7 confirms that this optimum position gives an optimum of thrust, despite the fact that the mass flow still grows with opening configuration (see Fig. 8). The mismatch between the flaps and the skin of the aircraft might be at the origin of this statement: an opening variation creates a displacement of the flaps that induces a backward facing step between flaps and skin for 125 and 150%, and a forward facing step for 50 and 75%. Figure 6 shows that a loss of thrust occurs even for pressure ratios corresponding to choked conditions, for which a supersonic jet is established. It can thus be concluded that the geometrical continuity between the flaps and the valve frame has an important impact on thrust generation.

The local static pressure measurements are now discussed. Figure 9 displays normalized static pressure distributions P/P_{tc} along the downstream flap at design opening configuration (100%) for several values of P_{Rc} ranging from 1.02 to 1.67. The pressure taps

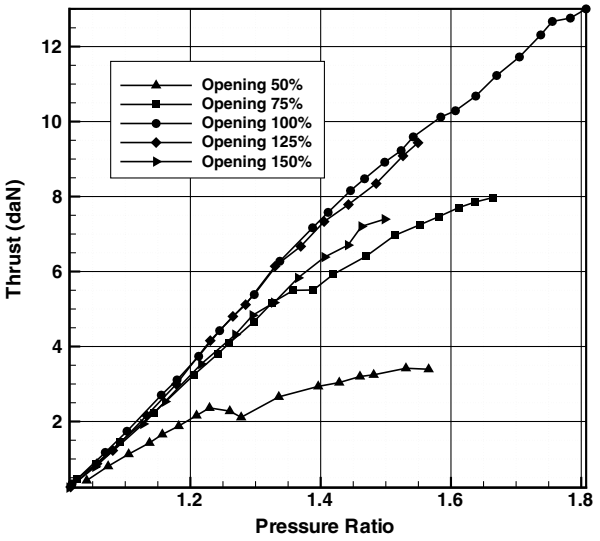

Fig. 6 Thrust vs cabin total pressure ratio.

position along the flap is given after their projection on the longitudinal axis (x direction in Fig. 3). In the first part of the distributions (before $x = 35$ mm), the flow moves across the channel created by the flaps of the valve and the pressure behaves in a classical way as in a convergent–divergent nozzle. The pressure decreases in the convergent and increases in the divergent for low P_{Rc} (1.02–1.25). Above those values, the pressure still decreases in the convergent, but the evolution is no more dependent on the pressure ratio. In the divergent part of the channel an additional expansion is produced, increasing with the pressure ratio. A brutal compression occurs at the end of this expansion zone. Actually, for low pressure ratios the flow is entirely subsonic and the minimum value of the curves located at $x = 0$ mm (third pressure tab) corresponds to the throat of the channel. For $P_{Rc} = 1.5$ choked conditions are reached. A supersonic flow takes place in a very small portion of the divergent part of the nozzle and a shock wave then compresses the flow just after pressure tab number 4 to reach external pressure conditions.

In the second part of the curves (after $x = 35$ mm, outside the ducted nozzle), a plateau is observed on the pressure distributions: pressure is constant and equals the external one. A small undershoot can be observed at $x = 108$ mm. This corresponds to the sharp angular variation of the wall at the trailing edge of the downstream flap that induces a local acceleration of the now subsonic jet.

An alternative analysis can be proposed by considering all the tested opening positions at the design value of the pressure ratio.

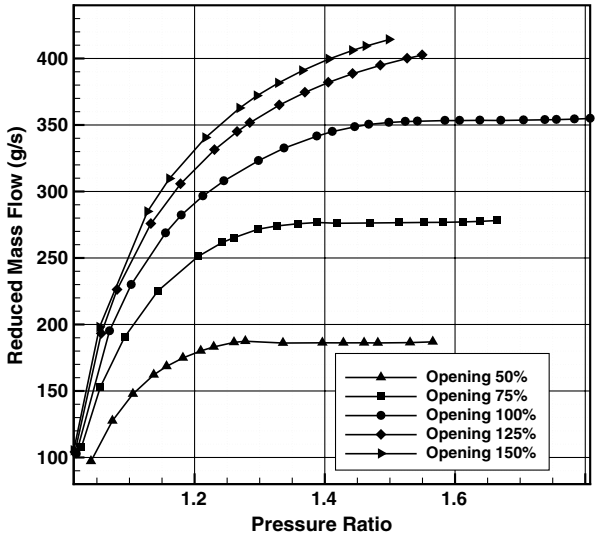

Fig. 5 Reduced mass flow rate vs cabin total pressure ratio.

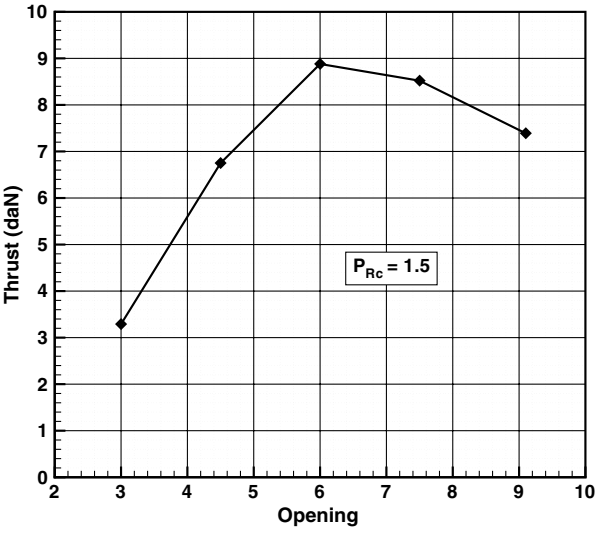

Fig. 7 Thrust vs valve opening for design pressure ratio.

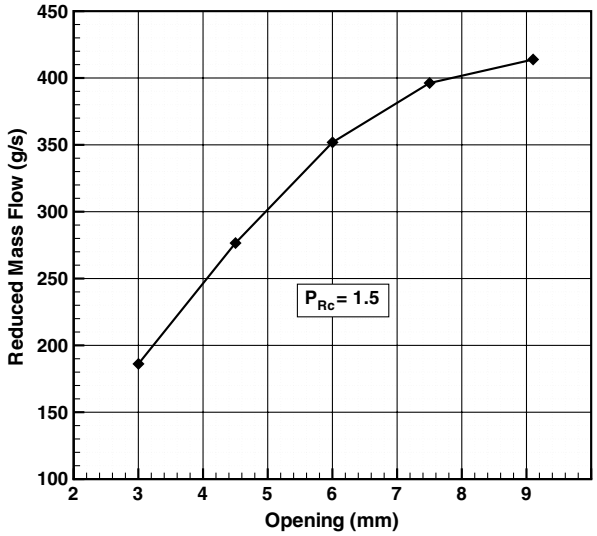

Fig. 8 Reduced mass flow rate vs valve opening for design pressure ratio.

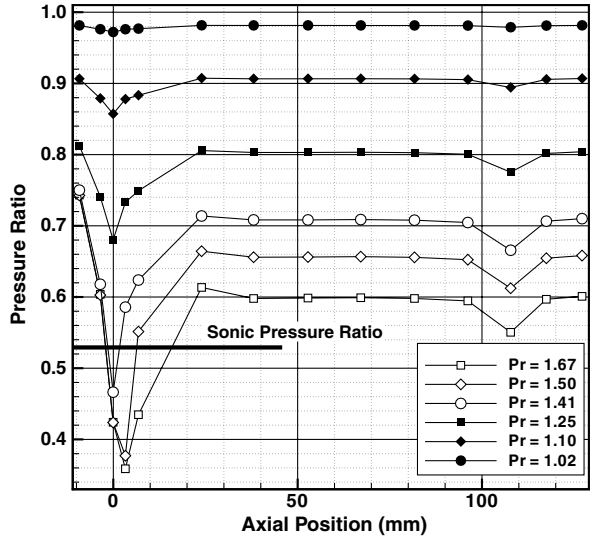

Fig. 9 Static pressure evolution on the downstream flap wall for various pressure ratios: opening 100%.

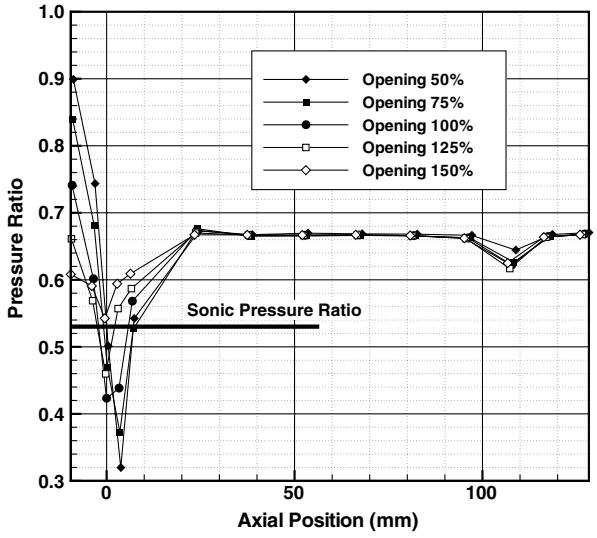

Fig. 10 Static pressure evolution on the downstream flap wall for various openings. Pressure ratio 1.5.

These curves are gathered in Fig. 10. A small shift can be observed in the axial position of the pressure tabs between the different curves because of the projection displacement of the pressure tabs position on the axial direction when changing the opening configuration (flap rotation). It is clear that the shock wave compression is higher when the opening is small. Energy losses are thus expected to be higher for small opening configurations.

These results attest the ability of the test rig to produce strong transonic jets. The thrust has been measured in that conditions, which are quite different from the actual flight conditions. However, they provided interesting informations about the outflow valve functioning. The main purpose of this experimental part is, however, to provide data on which validation of the numerical simulations is performed. This validation step is now detailed, together with the methodology used to run the simulations.

III. Numerical Simulations

A. Navier–Stokes Solver and Grid Generation

All the computations conducted in this research were achieved with the well-known Navier–Stokes solver FLUENT V6. Its reliability has been demonstrated by a great number of aerospace and industrial applications. The steady Reynolds-averaged Navier–Stokes (RANS) equations were solved. Several turbulence models were tested (*k*-epsilon, *k*-omega and Spalart–Allmaras), and results were similar between the different cases. The Spalart–Allmaras model [13] has been chosen because it involves only one transport equation (instead of two for *k*-epsilon and *k*-omega models), and it is thus numerically more efficient.

Figures 11 and 12 present the computational domain where two main parts (boxes) can be distinguished: *cabin* and *exterior*. Their sizes were chosen depending on the velocities occurring inside them. The cabin box is small because it is a low velocities portion of the domain. The exterior box that contains high velocities in cruise configuration is more important to get rid of numerical boundary effects in the zone of interest near the outflow valve. This computational domain is a half-model of the experimental test rig to take advantage of the symmetry of the problem. For all the runs, a

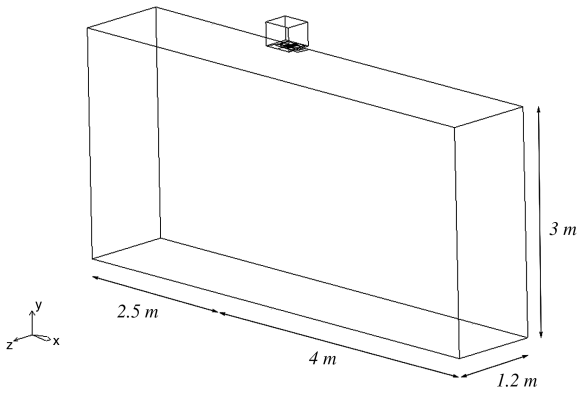

Fig. 11 Global 3-D computational domain.

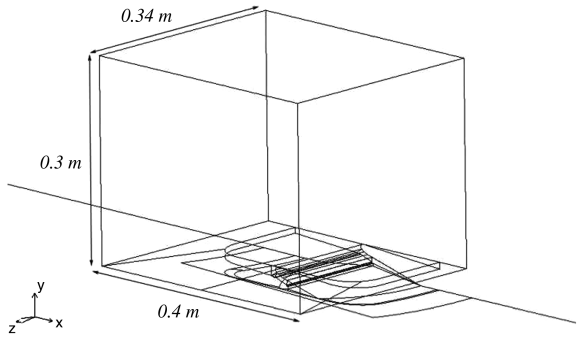

Fig. 12 Cabin box.

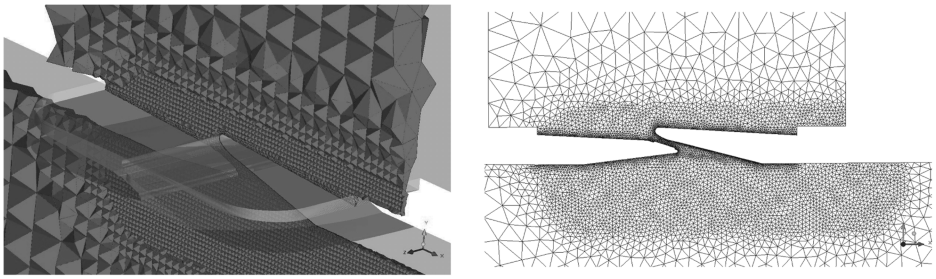

Fig. 13 Unstructured mesh near the outflow valve.

pressure inlet boundary condition was used for the upper and lateral sides of the cabin box and a pressure far field boundary condition was specified for the lateral and lower sides of the exterior box. A symmetry boundary condition was used for the surfaces located in the symmetry plane of the model while all others surfaces (flaps, lower side of cabin box, and upper side of exterior box) were set to walls.

Mesh generation was performed with ANSYS ICEMCFD V11. Because of the complexity of the model near the outflow valve, unstructured grids were used for this study. The grid of the half 3-D model contains 8,181,633 tetrahedral cells. Figure 13 provides a glimpse of the 3-D mesh and displays the cells repartition in the symmetry plane around the valve. The grid is refined in the region of the outflow valve where the exhaust jet takes place, near the skin of the flaps and in the tip wake region. Mesh sensibility has been investigated by performing several runs with three different grids involving 2, 4, and 8 million cells, respectively. No noticeable differences were found between the various cases concerning the pressure distributions along the valve channel, the flow pattern around the valve and the thrust value as well (at least for the two most refined grids). We chose to present the most refined 3-D case. Automatic mesh adaption has also been performed during the calculations to obtain correct values of the y^+ parameter (wall refinement) and also near shock waves (pressure gradient criterion) to better capture the physics of the flow. The 2-D cases correspond to a slice of the 3-D configuration along a plane perpendicular to the fuselage in the area of the outflow valve. Unstructured grids with 106,102 cells were used for these 2-D cases.

B. Computation of Thrust from CFD Data

In this work, thrust is computed using the integral formulation of the conservation of momentum law. For a steady flow, this allows to write for the fluid inside the volume limited by a surface S:

$$\int_S \rho \mathbf{V}(\mathbf{V}.\mathbf{n})\,\mathrm{d}S = \sum \mathbf{F}_{\text{ext}} \tag{3}$$

The shear and volume forces can reasonably be neglected in comparison to the momentum contribution. The projection of the previous equation on the x axis then leads to the thrust F:

$$F = F_x = \int_S \rho V_x^2\,\mathrm{d}S + \int_S P_s\,\mathrm{d}S \tag{4}$$

where S is the surface limiting a closed domain properly defined to reduce numerical diffusion errors.

C. Validation of the Numerical Procedure on the Ground Configuration

The validation procedure of the numerical simulations are conducted on the ground configuration, for which experimental data are available. This validation is performed for both 75 and 100% openings at design pressure ratio $P_{Rc} = 1.5$. We check the correspondence between experimental data and numerical results on both global parameters such as the mass flow rate across the outflow valve, as well as local information such as the static pressure distribution along the flaps.

1. *Mass Flow Rate*

When the experimental cabin static pressure of the chosen operating point is specified in the cabin box of the simulations, the numerical mass flow rate is overestimated compared with the experimental one. Two main factors were identified to explain this difference: pressure losses in the cabin box and throat section modification under pressure load.

In the experimental configuration, the mass flow enters the cabin box through a vertical pipe. For the stability of the numerical computations the same inlet condition could not be exactly reproduced. A pressure boundary condition has rather been imposed on the four lateral and the upper sides of the cabin. The actuator of the valve is moreover not included in the numerical model. For these two reasons, pressure losses inside the cabin box are more important in the experimental situation than in the numerical approach. Specific simulations were thus conducted to evaluate these losses for all the operating position range. We could estimate them to 4% of the inlet measured total pressure.

The real aircraft outflow valve used for the experiments introduces geometrical modifications under pressure load during test: the flaps reach their mechanical stop, which leads to a small throat section area reduction for the passing of the flow between the flaps. This is accepted in flight operation because the opening is automatically regulated to reach the cabin target pressure. These changes are mainly due to manufacturing defaults of the real equipment such as mechanical gaps, connecting rods and a nonparallelism of the flaps. This contribution can be quantified when the mass flow is choked because of the direct (linear) dependency of the mass flow with the sonic section area in this situation. This has been made for both 75 and 100% openings at design pressure ratios, and the throat section area reduction could be estimated to 16% of the theoretical one.

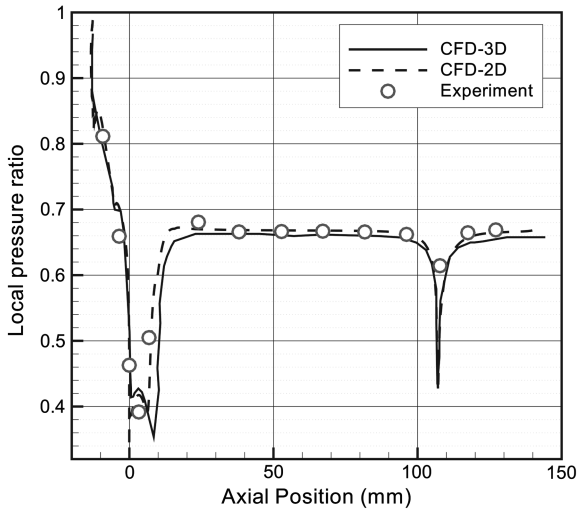

Fig. 14 Comparison between numerical and experimental pressure distributions along the downstream flap of the outflow valve: 100% opening configuration.

2. Pressure Distribution Along the Flaps

Attention also needs to be paid on the local pressure distribution along the flaps because it characterizes the way the nozzle formed by the channel between the flaps is working. For the operating points considered in this validation, experimental data display choked throat conditions, with an acceleration of the flow in the diverging part of the nozzle that allows to reach supersonic velocities. At the exit of the nozzle, an oblique shock wave occurs to recover external pressure conditions (cf., Sec. II.B). This leads to the pressure profiles along the downstream flap presented in Fig. 14 where both 2-D and 3-D CFD results are also displayed. The numerical pressure distributions are very close to experiments, which shows that the physics of the exhaust jet is properly reproduced by the simulations.

3. Procedure for the Calculation of the Outflow Valve Thrust from CFD

All the simulations dedicated to thrust computation were conducted taking into account the two corrective factors mentioned in Sec. III.C.1. To be as much representative as possible of the working of the outflow valve in the experiments, we made sure that the local numerical pressure distribution along the downstream flap matches the experimental data. To reach this operating point of the nozzle, however, CFD leads to overestimated mass flow rate as we explained previously (pressure losses in the cabin box and uncertainties concerning the effective throat section area in the experiments). As the thrust produced by the outflow valve is closely linked to the mass flow rate ejected through the nozzle between the flaps, we defined a procedure for the calculation of this thrust from CFD results as follows.

Our goal is to estimate the thrust corresponding to the experimental operating point (Q_{exp} at choked throat conditions) from the thrust calculated from 3-D CFD data (with the method described in Sec. III.B). Because we showed in the experiments that thrust grows quasi-linearly with mass flow rate (see Sec. II.B), this estimation can be made using the following simple model *3-D CFD corrected*:

$$F_{\text{corrected}} = \frac{Q_{\text{exp}} - Q_0}{Q_{\text{CFD}} - Q_0} * F_{\text{CFD}}$$

with $Q_0 = 260$ g/s for 100% opening. Q_0 is obtained by extrapolating the choked mass flow rate linear evolution at zero thrust. The results obtained by this methodology are presented in Table 2 and compared with the 1-D design model: $F_{1D} = Q * V * \cos(\xi)$.

It is important to recall here that the only purpose of this correction is to take into account the geometric differences between the CFD model and the experimental configuration, due to loading effects during the experiment. It does not affect the numerical calculation of the thrust, that we are here calibrating. Table 2 summarizes all the results.

Table 2 Comparison of measured and predicted thrust values for ground configuration and 100% opening

	Experiment	1-D model	2-D CFD	3-D CFD	3-D CFD corrected
Thrust, N	120	181	189	166	115
Mass flow rate, g/s	600	600	750	750	600

Table 3 Cruise thrust recovery of the outflow valve for 100 and 75% openings

		2-D CFD	3-D CFD	3-D CFD corrected
100% opening	Thrust, N	104	80	55.5
	Mass flow rate, g/s	353	364	291
75% opening	Thrust, N	69	58	40.2
	Mass flow rate, g/s	265	268	214

The thrust finally obtained with the 3-D CFD corrected model does not match exactly the experimental value, but it gives a correct estimation within 4% of the measured data. The 2-D CFD as well as the 1-D design model clearly overestimate the thrust. The same strategy has also been tested on the 75% opening configuration at ground conditions with the same accuracy, and it will now be used to provide an estimation of the thrust recovery of the outflow valve in cruise conditions for which no experimental data are available. The final step of the approach is now the simulation of the real flow condition, to obtain a thrust value.

IV. Final Results

In the last section of the paper, we use the numerical approach to fulfill the two objectives of this work: estimating the thrust provided by the outflow valve in cruise conditions and describing the main aerodynamic features of the flow.

A. Determination of Cruise Thrust Recovery

We first evaluate the thrust recovery of the outflow valve in cruise flight conditions ($P_{Rc} = 3$, with an external flow at Mach 0.777) by following the previous methodology validated in the ground configuration. The results of the different simulations are gathered in Table 3. The values corresponding to the *3-D CFD corrected* have been obtained by applying the same correction factor as in the ground configuration: the pressure loads on the outflow valve are indeed of the same order in both situations and the flaps have also reached mechanical stop in flight conditions. This results in the same throat section area reduction for both flows and thus to the same correction factor for the mass flow rate (which is a linear function of the section area in choked flows) and the thrust.

The recovery thrust generated by the outflow valve appears to be quite low and allows to expect at most a zero-weight equipment but not a real additional thrust. An improvement of the aircraft performance could, however, be obtained by using the exhaust jet to reduce the global drag of the air plane. This could be achieved by positioning the valve in the upsweep part of the fuselage to reduce the under-pressure zone generated in this portion of the geometry. Upsweep vortices intensity could then be lowered, as well as the global drag of the aircraft. The results reported in Table 3 also show that 2-D thrust is always slightly higher than its 3-D counterpart for a same mass flow rate. This can certainly be attributed to 3-D aerodynamics effects that will be highlighted in the next section.

B. Aerodynamic Behavior of the Outflow Valve

After having estimated the cruise thrust recovery, we try to shed some light on the aerodynamics of the outflow valve. Figure 15 displays Mach number and static pressure of the flow in the plane of symmetry of the valve in the vicinity of the flaps. The structure of the flowfield obeys the pressure repartition already described in Sec. II.B. We can notice the flow acceleration inside the converging part of the nozzle between the flaps, with sonic conditions at the throat, even if viscosity effects near the wall lead to an oblique sonic section which does not exactly correspond to the geometrical minimal section area. We can also visualize the oblique shock wave at the exit of the nozzle. Downstream of the shock, a supersonic jet exits the outflow valve. It remains attached to the downstream flap and undergoes an expansion at the trailing edge of the flap (junction with the fuselage corresponding to an aperture of the wall), immediately followed by a normal shock wave that compresses again the flow to external pressure conditions and brings back the jet to subsonic velocities.

In the previous section, 3-D effects were quantified regarding the recovery thrust of the outflow valve. They are the consequence of small aerodynamic side effects occurring at the tip of the flaps. These 3-D tip effects can be observed in Fig. 16 were the path lines of the flow are displayed. The rolling up of the path lines is not very pronounced, which allows to conclude that 3-D aerodynamic effects are small, even if they are discernible in thrust calculations. These visualizations also indicate that the expansion and the normal shock

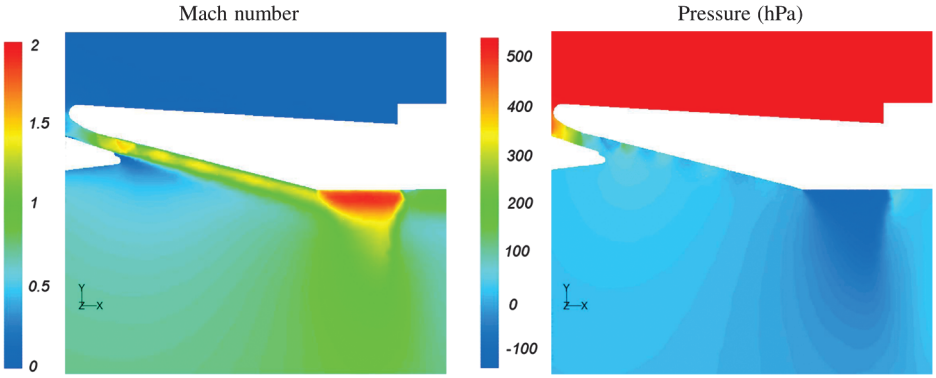

Fig. 15 Flow visualizations in the symmetry plane of the 3-D run: 6 mm opening configuration.

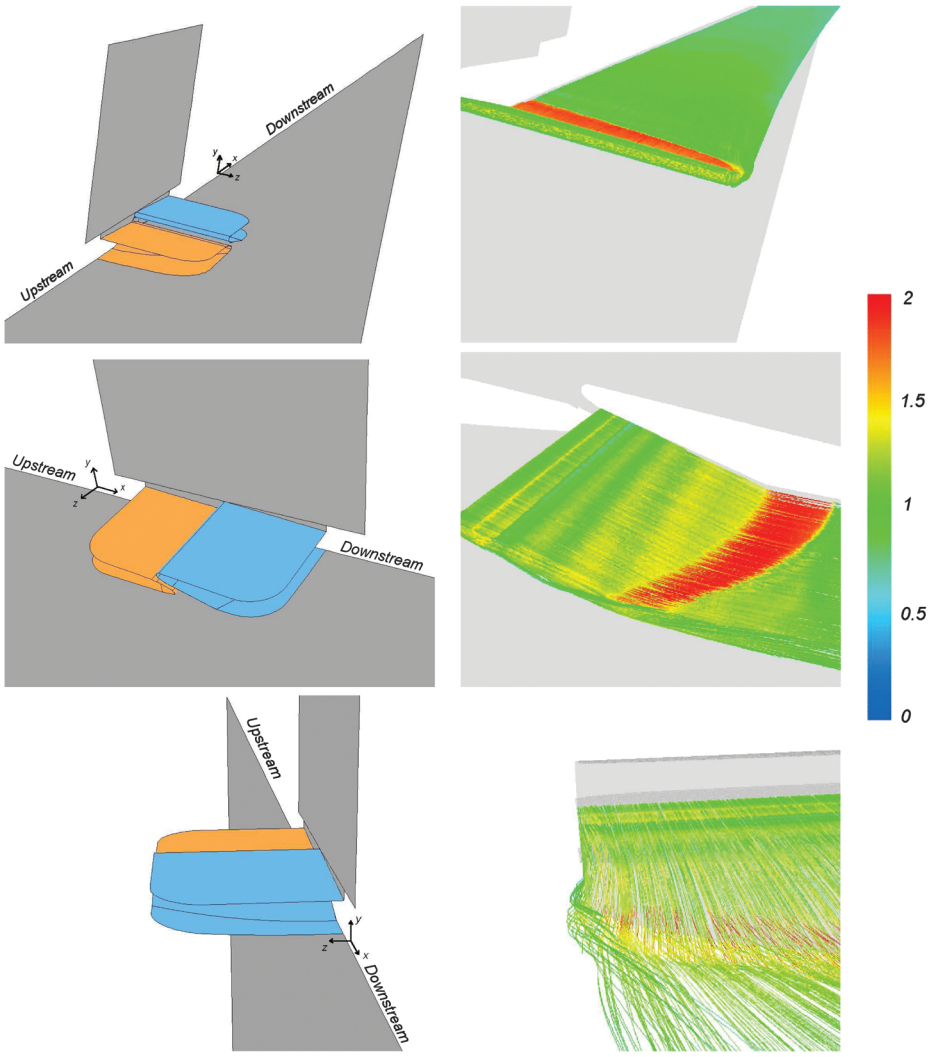

Fig. 16 Angle of view (left) and path lines (right) of the flow exiting the valve colored by the Mach number: 3-D run, 6 mm opening configuration.

wave occurring at the junction between the downstream flap and the fuselage are curved because of the curvature of the flap trailing edge in the spanwise direction.

V. Conclusions

This paper summarizes the major results of a mixed experimental/numerical study of a flapped outflow valve. Validation of the numerical approach was first conducted by comparing experimental data and numerical results on a ground configuration: small pressure ratio between the cabin and the external domain without flow outside the cabin, generating transonic conditions in the exhaust jet. Numerical results compared well with experiments, provided some adjustments that were introduced to take into account pressure losses in the experimental test rig and geometric modifications of the throat of the flaps nozzle due to pressure loads. Correction factors were then drawn from this validation procedure and were applied to additional numerical results obtained at cruise conditions for which no experimental data were available. This allowed to provide a reliable cruise thrust recovery value for this type of equipment, which had never been done before. Given the order of magnitude of the result, we could conclude that the thrust recovery is very small: this type of

outflow valve does not provide a significant additional thrust. The drag reduction action of this equipment by blowing in the upsweep region compared with the actual thrust generated has now to be evaluated. The aerodynamic behavior of the flow was also highlighted and small 3-D effects could be observed on the sides of the flaps when the flow leaves the valve. Geometry modifications of the valve could then be investigated to see if thrust recovery (or drag reduction) can be improved.

Acknowledgments

The authors wish to thank Liebherr Aerospace Toulouse S.A. for the financial support, and particularly Christine Stephan for her technical contribution.

References

[1] Mauldin, L. F., "Cabin Pressure Outflow Valve," United States Patent No. 2.846.934, 1958.

[2] Fejtek, I., Waller, G., and Wong, R., "Computational Study of the Flowfield of an Aircraft Outflow Valve," *23rd AIAA Applied Aerodynamics Conference*, AIAA, Reston, VA, 2005.

[3] Emmons, F. R., "Aircraft Pressurization Outflow Valve," United States Patent No 3.426.984, 1969.

[4] Chuang, K. S., Ho, Y., and Opdycke, S. R., "Aircraft Cabin Outflow Valve Including Aft Door Modified for Noise Suppression," United State Patent No. 6.116.541, 2000.

[5] Smid, E., Spalart, P. R., and Breard, C. C., "Outflow Valve Noise Analysis Using Two-Dimensional U-RANS CFD,"*13th AIAA/CEAS Aeroacoustics Conference (28th AIAA Aeroacoustics Conference)*, AIAA, Reston, VA, 2007.

[6] Dash, S. M., and Wolf, D. E., "Interactive Phenomena in Supersonic Jet Mixing Problems. Part 1: Phenomenology and Numerical Modeling Techniques," *AIAA Journal*, Vol. 22, No. 7, 1984, pp. 905–913. doi:10.2514/3.8707

[7] Dash, S. M., and Wolf, D. E., "Interactive Phenomena in Supersonic Jet Mixing Problems. Part II: Numerical Studies," *AIAA Journal*, Vol. 22, No. 10, 1984, pp. 1395-1404. doi:10.2514/3.48580

[8] Beresh, S. J., Henfling, J. F., Erven, R. J., Spillers, R. W., "Crossplane Velocimetry of a Transverse Supersonic Jet in a Transonic Crossflow," *AIAA Journal*, Vol. 44, No. 12, 2006, pp. 3051–3061. doi:10.2514/1.22311

[9] Beresh, S. J., Henfling, J. F., and Erven, R. J., "Surface Measurements of a Supersonic Jet in Subsonic Compressible Crossflow for the Validation of Computational Models," Sandia National Lab., Technical Rept. SAND2002-1890, Albuquerque, NM, 2002. doi: 10.2172/806698

[10] Chocinski, D., Leblanc, R., and Hachemin, J.-V., "Experimental/ Computational Investigation of Supersonic Jet in Subsonic Compressible Crossflow,"*35th Aerospace Sciences Meeting and Exhibit*, AIAA, Reston, VA, 1997.

[11] Plesniak, M. W., and Cusano, D. M., "Scalar Mixing in a Confined Rectangular Jet in Crossflow," *Journal of Fluid Mechanics*, Vol. 524, 2005, pp. 1–45. doi: 10.1017/S0022112004001132

[12] Weston, R. P., and Thames, F. C., "Properties of Aspect Ratio 4.0 Rectangular Jets in Subsonic Crossflow," *Journal of Aircraft*, Vol. 16, No. 10, 1979, pp. 701–707. doi:10.2514/3.58592

[13] Spalart, P. R., and Allmaras, S. R., "A One-Equation Turbulence Model for Aerodynamic Flows," *30th Aerospace Sciences Meeting and Exhibit*, AIAA Paper 92-0439, 1992.